

Lasing action in water vapor induced by ultrashort laser filamentation

Shuai Yuan, Tiejun Wang, Yoshiaki Teranishi, Aravindan Sridharan, Sheng Hsien Lin, Heping Zeng, and See Leang Chin

Citation: [Applied Physics Letters](#) **102**, 224102 (2013); doi: 10.1063/1.4809585

View online: <http://dx.doi.org/10.1063/1.4809585>

View Table of Contents: <http://scitation.aip.org/content/aip/journal/apl/102/22?ver=pdfcov>

Published by the [AIP Publishing](#)

Articles you may be interested in

[Effects of nanosecond-duration laser prepulses on solid targets](#)

J. Appl. Phys. **97**, 103303 (2005); 10.1063/1.1904719

[Femtosecond-irradiation-induced refractive-index changes and channel waveguiding in bulk Ti 3 + : Sapphire](#)

Appl. Phys. Lett. **85**, 1122 (2004); 10.1063/1.1781737

[Gain-switched, all-acousto-optic, femtosecond pulse amplifier](#)

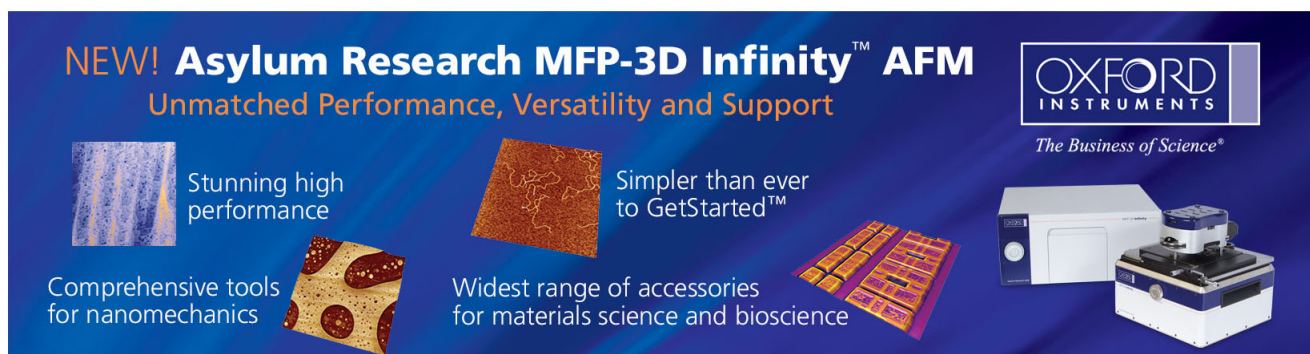
Rev. Sci. Instrum. **74**, 4961 (2003); 10.1063/1.1619581

[Short pulsed laser machining: How short is short enough?](#)

J. Laser Appl. **11**, 268 (1999); 10.2351/1.521902

[Construction of a subpicosecond double-beam laser photolysis system utilizing a femtosecond Ti:sapphire oscillator and three Ti:sapphire amplifiers \(a regenerative amplifier and two double passed linear amplifiers\), and measurements of the transient absorption spectra by a pump-probe method](#)

Rev. Sci. Instrum. **68**, 4364 (1997); 10.1063/1.1148398

The advertisement for the Asylum Research MFP-3D Infinity AFM features a dark blue background with white and yellow text. At the top left, it reads 'NEW! Asylum Research MFP-3D Infinity™ AFM' in large white letters, followed by 'Unmatched Performance, Versatility and Support' in yellow. The Oxford Instruments logo is in the top right corner, with the tagline 'The Business of Science®' below it. The central part of the ad is divided into four quadrants, each with an image and text: 'Stunning high performance' with a blue textured image; 'Simpler than ever to GetStarted™' with a brown textured image; 'Comprehensive tools for nanomechanics' with a yellow textured image; and 'Widest range of accessories for materials science and bioscience' with a yellow textured image. On the right side, there is a photograph of the AFM instrument itself, a white and blue device with a sample stage.

Lasing action in water vapor induced by ultrashort laser filamentation

Shuai Yuan,^{1,2} Tiejun Wang,^{1,3} Yoshiaki Teranishi,⁴ Aravindan Sridharan,¹ Sheng Hsien Lin,⁵ Heping Zeng,^{2,6,a)} and See Leang Chin^{1,b)}

¹Centre d'Optique, Photonique et Laser (COPL) and Département de physique, de génie physique et d'optique, Université Laval, Québec, Québec G1V 0A6, Canada

²State Key Laboratory of Precision Spectroscopy, East China Normal University, Shanghai 200062, China

³State Key Laboratory of High Field Laser Physics, Shanghai Institute of Optics and Fine Mechanics, Chinese Academy of Sciences, Shanghai 201800, China

⁴Institute of Physics, National Chiao-Tung University, Hsin-Chu 300, Taiwan and Physics Division, National Center for Theoretical Sciences, Hsin-Chu 300, Taiwan

⁵Department of Applied Chemistry, National Chiao-Tung University, Hsin-Chu 300, Taiwan and Institute of Atomic and Molecular Sciences, Academia Sinica, Taipei 106, Taiwan

⁶Shanghai Key Laboratory of Modern Optical System, Engineering Research Center of Optical Instrument and System, Ministry of Education, School of Optical-Electrical and Computer Engineering, University of Shanghai for Science and Technology, Shanghai 200093, China

(Received 7 March 2013; accepted 19 May 2013; published online 3 June 2013)

The water vapor fluorescence in air from filaments generated by intense ultrashort Ti:sapphire laser pulses is experimentally studied. The backscattered fluorescence from OH shows an exponential increase with increasing filament length, indicating amplified spontaneous emission. By measuring the intensity inside the filament and the fluorescence intensity of OH, a high degree of nonlinearity is obtained, indicating a highly nonlinear field dissociation of H₂O molecule.

© 2013 AIP Publishing LLC. [<http://dx.doi.org/10.1063/1.4809585>]

Self-guided propagation of ultrashort intense laser pulse in air is demonstrated to induce a filamentation channel,^{1,2} which has attracted a lot of scientific interests. Filamentation is known as a dynamic equilibrium between Kerr self-focusing and defocusing by the self-generated plasma produced by multiphoton/tunnel ionization of air molecules.^{1–6} For short filament (<5 cm), intensity clamping produces a self-stabilized high peak intensity inside the filament of the order of $\sim 5 \times 10^{13}$ W/cm², while longer filaments might lead to intensity spikes.^{7,8} Both of them can be beneficial for a lot of nonlinear effects, such as remote sensing,^{9–11} molecular alignment,^{12,13} harmonic generation,^{7,8,14,15} etc. Inside filament, most molecules undergo multiphoton/tunneling ionization and fragmentation, which excites the ions and fragment molecules into some highly excited states, resulting in the emission of characteristic fingerprint fluorescence.^{16,17}

Luo *et al.*¹⁸ have observed that the spontaneous emission from N₂ molecules and ions become amplified as it propagates back along the filament. The amplified spontaneous emission (ASE) is characterized as ASE lasing. More recently, lasing action from filaments was shown to operate at both ~ 391 and 337 nm in molecular nitrogen^{19,20} and at ~ 845 nm in atomic oxygen.²¹ In this work, we investigated the backscattered fluorescence of OH from water vapor in air, from the filament which is generated by a femtosecond Ti:sapphire laser pulse. The dependence of the fluorescence of OH on the filament length shows clear evidence of ASE. Besides, by measuring the intensity inside the filament and fluorescence intensity of OH, a high degree of nonlinearity is obtained.

The experiments were done by using a 12 mJ/50 fs, 10 Hz Ti:sapphire laser beam. The schematic of the experimental setup is illustrated in Fig. 1(a). The laser beam was focused by

a lens of 42 cm focal length. A dichroic mirror (M1, 7.5 cm in diameter) with high reflectivity at 800 nm and 50% transmission from 300 nm to 315 nm was used right after the lens to reflect the beam at 45° incidence angle. A 5-cm-long filament was created roughly 35 cm after the mirror (M1) in air. A beaker with open area of 15 cm in diameter was placed 4 mm under the filament. The beaker was fully filled with distilled water, in order to create an environment with a water vapor concentration of $\sim 2\%$ at room temperature (22 °C) according to our measurement in Ref. 22. The backscattered fluorescence from the filament zone was collected after the dichroic mirror (M1) with a fused-silica lens (5.08 cm in diameter, 10 cm focal length) and sent to an intensified charge coupled device (ICCD)-gated spectrometer (Acton Research Corporation, SpectraPro-500i) through a fiber coupler. The fluorescence from the side was obtained by imaging the filament onto and parallel to the 100 μ m-wide slit of the same ICCD-gated spectrometer using two identical fused-silica lenses ($\Phi 5.08$ cm $f = 10$ cm) and one periscope. A grating of 1200 grooves/mm (blazed at 500 nm) was used. All the results shown in this paper are averaged over 1000 laser shots.

Fluorescence coming from the water vapor was found in the range of 306–309 nm as shown by the black curve in Fig. 1(b), at room temperature (22 °C) and with 2 mJ of the pump pulse energy. The fluorescence was identified as OH* radiation from $A^2\Sigma^+ \rightarrow X^2\Pi$.^{22,23} The fluorescence from molecular N₂ was also observed around the peak of 315 nm as shown in Fig. 1(b). To check whether the fluorescence of N₂ has any effect on the typical OH radiation at 308.9 nm, another trial experiment was carried out. The beaker filled with water was replaced by a gas nozzle, which continuously provided a dry air blow to reduce the amount of water vapor in air. The spectrum of the back-scattered fluorescence from the filament was detected then. The result is shown as the blue dashed curve in Fig. 1(b). In this case, the signal around

^{a)}Electronic address: hpzeng@phy.ecnu.edu.cn

^{b)}Electronic address: slchin@phy.ulaval.ca

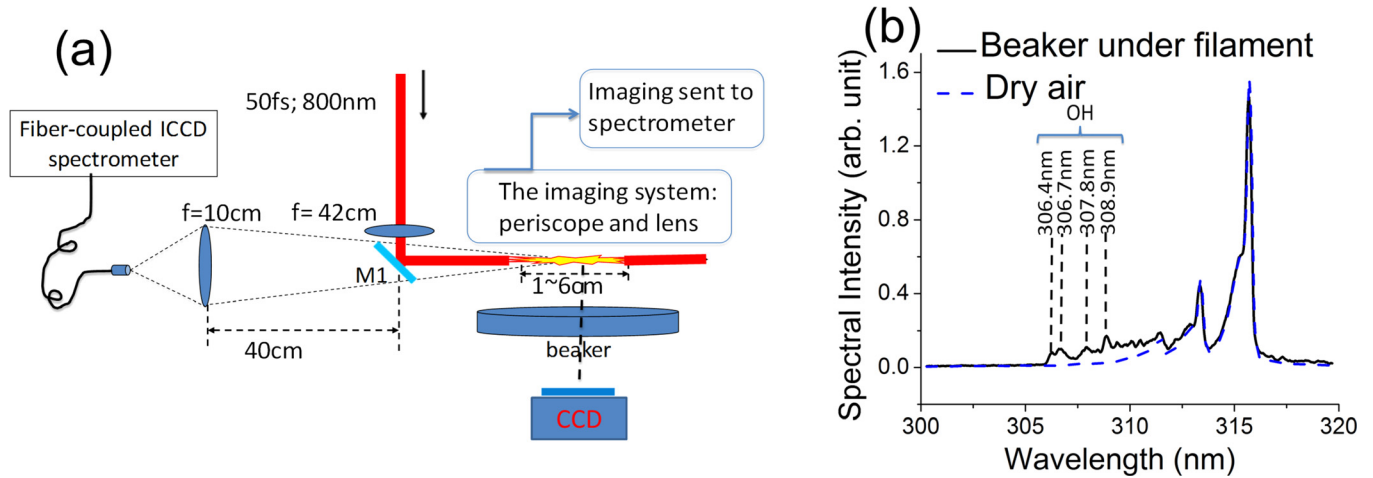


FIG. 1. (a) Schematic layout of experimental setup and (b) typical spectrum in the range of 300–320 nm for filament-induced fluorescence of water vapor in air. The spectrum was taken at room temperature of 22 °C and filament-to-water surface of 4 mm.

308.9 nm which corresponds to the OH fluorescence decreases to the noise level, i.e., both N₂ and O₂ molecules have no contribution to the fluorescence of OH around 308.9 nm. In this paper, the spectral peak intensities of 308.9 nm from OH were chosen as the OH fluorescence.

The OH fluorescence in the backward and side directions was measured with the gated-ICCD spectrometer under different input pump pulse energy. A CCD was employed to image the filament from the side [see Fig. 1(a)] in order to measure the length of the filament. The result is shown in Fig. 2(a) (detected from the backward direction) and Fig. 2(b) (detected from the side). In Fig. 2(a), the backscattered OH fluorescence increases exponentially as the filament length increases, while in Fig. 2(b), the OH fluorescence from the side has a linear dependence with the filament length. If the OH fluorescence signal is incoherent, OH fluorescence emission detected in the backward and side directions should give similar results. However, in our experiment, the on-axis backward OH fluorescence signal increases much faster

(increase exponentially) with the filament length than the one detected from the side (increase linearly). This indicates amplified spontaneous emission. The ASE can be expressed as

$$I \propto P = \int_0^L P_s e^{g(l)l} dl = \begin{cases} \frac{P_s}{\bar{g}} (e^{\bar{g}L} - 1) & (1a) \\ \frac{P_s}{\bar{g}} \times \bar{g}L = P_s L & (1b) \end{cases}$$

(with amplification),
(when $\bar{g}L \ll 1$),

where I is the intensity of the spontaneous emission, P the spontaneous emission power, P_s the spontaneous emission power per unit length, and L the effective length of the gain medium, which roughly equals to the length of the filament. $g(l)$ is defined as the optical gain coefficient, which is a function of the relative position l inside the filament. \bar{g} is the effective gain coefficient over the filament length. In our

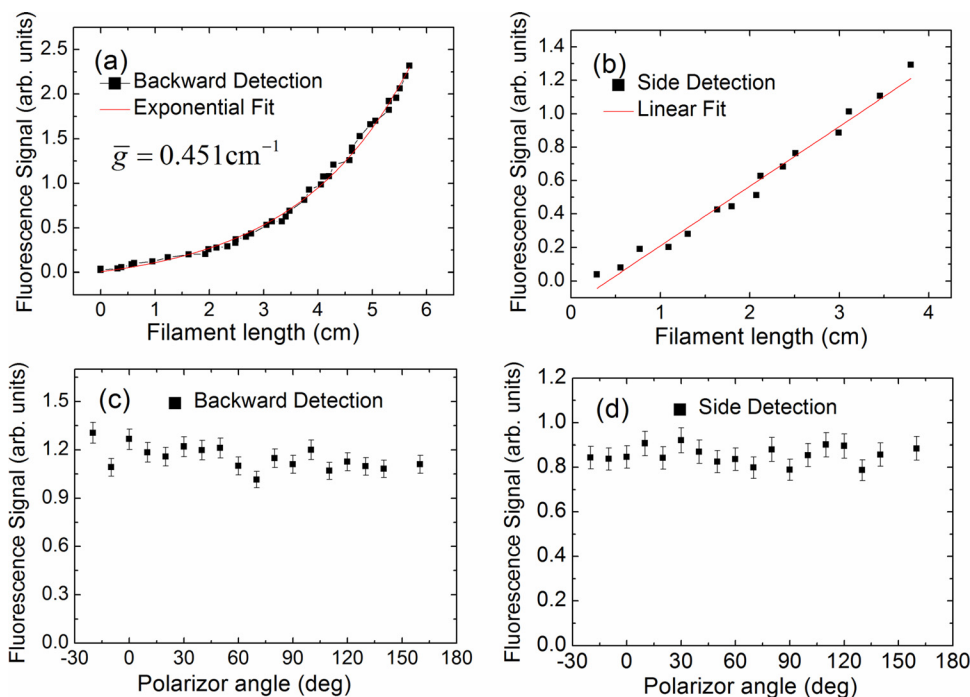


FIG. 2. The fluorescence intensity of OH at 308.9 nm versus the filament length. The fluorescence is recorded in backward (a) and side (b) direction. The laser beam is focused by an external focusing lens ($f = 42$ cm). The solid line in (a) is the gain curve calculated with Eq. (1a). The polarization property of the fluorescence in backward and side directions is shown in (c) and (d), respectively.

experiment, the maximum length of the filament is 5 cm. In this sense, due to intensity clamping, we assume the intensity inside the filament is uniform and consider the filament zone approximately as a cylinder, meaning that the optical gain $g(l)$ has little deviation from the effective gain coefficient \bar{g} over the filament length. In Eq. (1a), when the spontaneous fluorescence is amplified along the gain medium, the integrated fluorescence shows an exponential dependence with the length L of the gain medium (filament), which corresponds to the result in Fig. 2(a). By applying Eq. (1a), the experimental curve in Fig. 2(a) can be fitted with an effective gain coefficient of 0.451 cm^{-1} . In Fig. 2(b), the OH fluorescence is proportional to the filament length, since the fluorescence detected from the side only sees the gain along the very small filament cross section (roughly $100 \mu\text{m}$), which is a short distance. The value of the gain along the cross section should have the same magnitude as the effective gain coefficient detected from the backward direction (0.451 cm^{-1}). Therefore, in this case, the product of the gain (assuming $\bar{g} = 0.451 \text{ cm}^{-1}$) and the length of the gain medium ($L = 100 \mu\text{m}$) are negligibly small ($\bar{g}L \ll 1$), which corresponds to Eq. (1b). As a result, the integrated OH fluorescence from the side is just the sum of the emission from all the small unit lengths along the filament, in accordance with our results in Fig. 2(b). The absolute value of the OH fluorescence intensity in Figs. 2(a) and 2(b) is not comparable, since the measurements from the side and the backward direction employed different techniques. The polarization of the fluorescence in the backward/side direction was measured by rotating a polarizer placed just before the fiber head (backward direction) or the slit of the spectrometer (side). Both of them are randomly polarized as shown in Figs. 2(c) and 2(d). The isotropic polarization and the difference between the gain in backward and side directions provide strong evidences for ASE lasing.

In order to understand the physics of the lasing action and the dissociation process, an energy diagram was plotted and shown in Fig. 3(a), with 12.6 eV as the ionization

potential (IP) of H_2O molecule. There are two distinctive dissociation channels for H_2O molecule below the ionization potential related to OH generation:^{24,25} one dissociating into $H(^2S) + OH(X^2\Pi)$, giving rise to H and OH fragments in the ground states,²⁵ and the other dissociating into $H(^2S) + OH(A^2\Sigma^+)$, resulting in H in the ground state and OH in the excited state. The threshold energy of 9.136 eV for exciting this channel comes from Refs. 24–26, where single vacuum ultraviolet (VUV) photons were used in the dissociation of H_2O . The OH* fluorescence at 306–309 nm in this experiment was identified as the transition from $A^2\Sigma^+ \rightarrow X^2\Pi$.^{22,23} If the dissociation channels above the ionization potential (12.6 eV) happened, the excited state of H, named H*, would be generated together with OH*(A) [see Fig. 3(a)]. However, during the experiment, we did not observe any spectral line from the Balmer series, which corresponds to the H* radiation. Thus, it can be assumed that inside the filament the water vapor molecules can be dissociated through the channel $H(^2S) + OH(A^2\Sigma^+)$. The transition from OH ($A^2\Sigma^+ \rightarrow X^2\Pi$) emits fluorescence 306–309 nm, having a peak at 308.9 nm.

In this sense, different from previous work that molecular H_2O is dissociated by single UV photon, the dissociation of H_2O molecule through $H(^2S) + OH(A^2\Sigma^+)$ by infrared photon at 800 nm is a multiphoton or highly nonlinear field interaction process. In order to prove our assumption, one supplementary experiment was carried out by measuring the intensity inside the filament and OH fluorescence emission at different input pump pulse energy. Note that although the intensity is supposed to be uniformed along the filament, if the pump power is below or near the critical power for self-focusing ($\sim 10 \text{ GW}$ in air), the intensity inside the filament would change by varying the pump pulse energy. During this experiment, the lens $f = 42 \text{ cm}$ in Fig. 1(a) was replaced by another lens with $f = 50 \text{ cm}$. At different pump pulse energy, the effective filament length was imaged into the ICCD-gated spectrometer from the side. The intensity at every

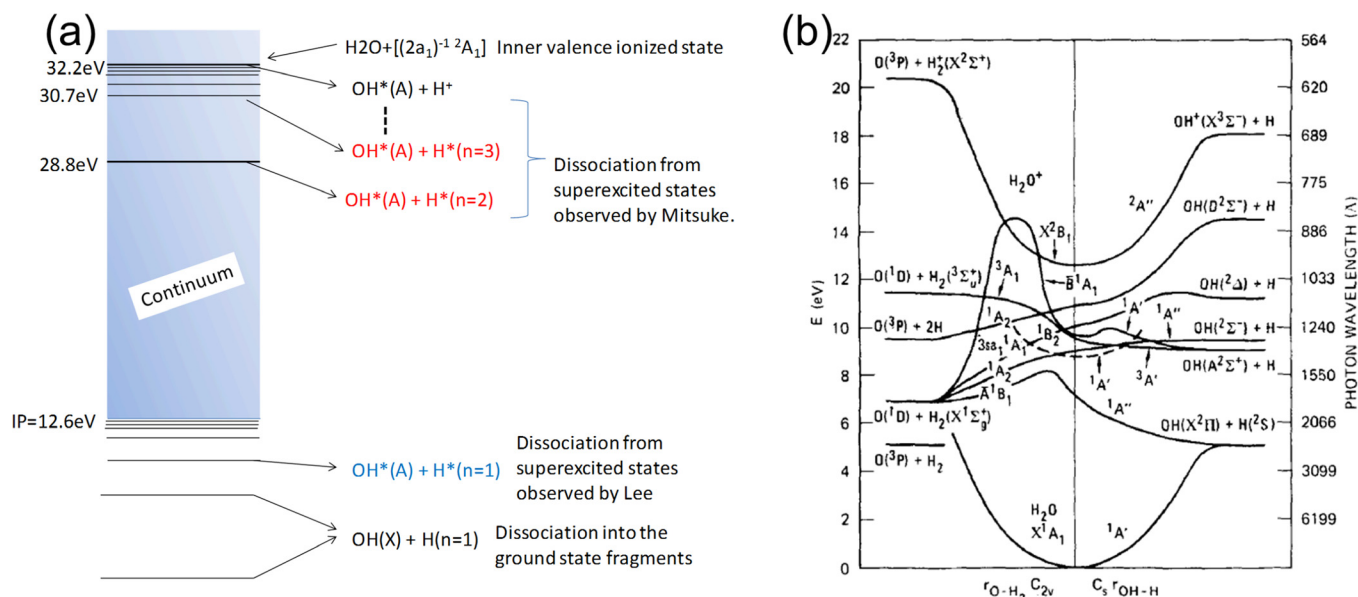


FIG. 3. (a) Schematic energy diagram for molecular H_2O . (b) Correlation diagram for the electronic states of H_2O relevant to the current observation. This diagram is given by Tsurubuchi.²⁸ The photon wavelengths corresponding to excitation energies are indicated. Fig. 3(b) is adapted with permission from Ref. 24 (AIP, 1980), image courtesy of Lee, SRI International, California.

small unit lengths (0.15 mm by calibration) along the effective filament length was calculated according to Eq. (13) in Ref. 27, by measuring the ratio of the spectral intensity of two nitrogen fluorescence lines, 391 and 337 nm. Then, the peak intensity was selected and the intensity of OH fluorescence at this unit length was recorded. We plotted the OH fluorescence versus the peak intensity over this unit length. The result is shown in a log-log plot in Fig. 4, with a slope of 6.6. The slope does not correspond to an exact number of photons. However, in Fig. 3(b) around 9 eV (roughly 6 photon energy) a high density of states exists. These states could be coupled by the strong field and dissociating into the $H(^2S) + OH(A^2\Sigma^+)$ channel. The fluorescence from $OH(A^2\Sigma^+)$ is attributed to the pumping to these excited states. The excitation probability into these coupled excited states may have the slope of 6 or 7 (or some other non-integer values). In this sense, the slope 6.6 which is observed in the experiment is the mixture of the contribution from various excited states.

Thus, it is reasonable to conclude that the gain in the fluorescence of OH comes from the dissociation channel $H_2O + nh\nu \rightarrow H(^2S) + OH(A^2\Sigma^+)$ [see Fig. 3(a)]. Here, n indicates the mixture of the contribution from various excited states and not an exact number of photons. However, if the other lower lying channel $H_2O + n'h\nu \rightarrow H(^2S) + OH(X^2\Pi)$ which would give rise to OH (X) fragments in the ground state were also possible, it would reduce the population inversion in the ensemble of OH population. We would argue that such latter channel would be less probable. Under strong broadband femtosecond laser field excitation, many molecular states might have been coupled by the field. The higher the density of states is, the more probable the coupling could be. In the experiment, the strong field was set by intensity clamping in the air filament where the intensity was of the order of 5×10^{13} W/cm². According to Fig. 3(b), the region of higher density of states is around 9 eV, which would decay into the channel $H_2O + nh\nu \rightarrow H(^2S) + OH(A^2\Sigma^+)$. Hence, the excitation of this channel would be more probable. Since OH* is created directly, its population is naturally inverted, and thus ASE lasing occurs.

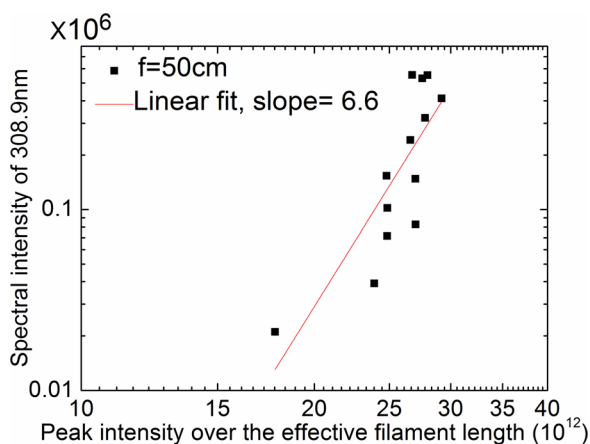


FIG. 4. Fluorescence intensities of OH 308.9 nm lines as a function of the peak intensity over the effective filament length, shown in log-log scale, with 50 cm focal length lens. The slope is 6.6.

In summary, an exponential variation of the backscattered fluorescence from water vapor with increasing filament length was experimentally observed. This indicates that the fluorescence has been amplified while it propagates back along the filament. It opens up possibilities for the investigation on lasing action of water vapor through filament, since it exhibits similar characteristics as the N₂ molecules and ions. For example, we might also expect that the harmonic-seeded remote laser emission²⁰ can be operated in water vapor molecules as well. Besides, different from previous work using UV pulse to dissociate molecular H₂O through single photon process, the molecular H₂O is dissociated by infrared pulse under strong field process inside a filament. The detailed underlying physics of the dissociation through filamentation awaits to be explored.

The authors thank Ali Azarm and Huailiang Xu for fruitful scientific discussions. This work was supported in part by NSERC, Canada Research Chair, the Canada Foundation for Innovation, the Canadian Institute for Photonics Innovation, le Fonds Québécois pour la Recherche sur la Nature et les Technologies, International Cooperation Project from Shanghai Science and Technology commission, International Cooperation Project for Ministry of Science and Technology in China, and Chinese Government Scholarships for Construction of High Level University graduate program.

¹S. L. Chin, *Femtosecond Laser Filamentation*, Springer Series on Atomic, Optical and Plasma Physics Vol. 55 (Springer, 2010).

²A. Couairon and A. Mysyrowicz, *Phys. Rep.* **441**, 47 (2007).

³S. L. Chin, *Phys. Can.* **60**, 273–281 (2004).

⁴L. Bergé, S. Skupin, R. Nuter, J. Kasparian, and J. P. Wolf, *Rep. Prog. Phys.* **70**, 1633 (2007).

⁵S. L. Chin, S. A. Hosseini, W. Liu, Q. Luo, F. Théberge, N. Aközbek, A. Becker, V. P. Kandidov, O. G. Kosareva, and H. Schroeder, *Can. J. Phys.* **83**, 863 (2005).

⁶J. Kasparian and J. P. Wolf, *Opt. Express* **16**, 466 (2008).

⁷M. B. Gaarde and A. Couairon, *Phys. Rev. Lett.* **103**, 043901 (2009).

⁸D. S. Steingrube, E. Schulz, T. Binhammer, M. B. Gaarde, A. Couairon, U. Morgner, and M. Kovačev, *New J. Phys.* **13**, 043022 (2011).

⁹G. Heck, E. J. Judge, J. Odhner, M. Plewiczki, and R. J. Levis, in *paper presented at GomacTech Digest Conference, Orlando, FL, 2009*, <http://www.temple.edu/capr/publications/PDFs/gomacLevisPaper-010709.pdf>.

¹⁰J. Kasparian, M. Rodriguez, G. Méjean, J. Yu, E. Salmon, H. Wille, R. Bourayou, S. Frey, Y. B. André, A. Mysyrowicz, R. Sauerbrey, J. P. Wolf, and L. Wöste, *Science* **301**, 61 (2003).

¹¹H. L. Xu, G. Méjean, W. Liu, Y. Kamali, J. F. Daigle, A. Azarm, P. Simard, P. Mathieu, G. Roy, J. R. Simard, and S. L. Chin, *Appl. Phys. B* **87**, 151 (2007).

¹²S. Varma, Y. H. Chen, and H. M. Milchberg, *Phys. Rev. Lett.* **101**, 205001 (2008).

¹³J. Wu, H. Cai, H. P. Zeng, and A. Couairon, *Opt. Lett.* **33**, 2593 (2008).

¹⁴X. Yang, J. Wu, Y. Peng, Y. Tong, S. Yuan, L. Ding, Z. Xu, and H. P. Zeng, *Appl. Phys. Lett.* **95**, 111103 (2009).

¹⁵F. Théberge, N. Aközbek, W. Liu, J. Fillion, and S. L. Chin, *Opt. Commun.* **276**, 298 (2007).

¹⁶S. L. Chin, H. L. Xu, Q. Luo, F. Théberge, W. Liu, J. F. Daigle, Y. Kamali, P. T. Simard, J. Bernhardt, S. A. Hosseini, M. Sharifi, G. Méjean, A. Azarm, C. Marceau, O. Kosareva, V. P. Kandidov, N. Aközbek, A. Becker, G. Roy, P. Mathieu, J. R. Simard, M. Châteauneuf, and J. Dubois, *Appl. Phys. B* **95**, 1 (2009).

¹⁷H. L. Xu and S. L. Chin, *Sensors* **11**, 32 (2011).

¹⁸Q. Luo, W. Liu, and S. L. Chin, *Appl. Phys. B* **76**, 337 (2003).

¹⁹P. R. Hemmer, R. B. Miles, P. Polynkin, T. Siebert, A. V. Sokolov, P. Sprangle, and M. O. Scully, *Proc. Natl. Acad. Sci. U.S.A.* **108**, 3130 (2011).

²⁰J. Yao, B. Zeng, H. Xu, G. Li, W. Chu, J. Ni, H. Zhang, S. L. Chin, Y. Cheng, and Z. Xu, *Phys. Rev. A* **84**, 051802 (2011).

- ²¹A. Dogariu, J. B. Michael, M. O. Scully, and R. B. Miles, *Science* **331**, 442 (2011).
- ²²T. Wang, H. Xu, J. F. Daigle, A. Sridharan, S. Yuan, and S. L. Chin, *Opt. Lett.* **37**, 1706 (2012).
- ²³R. W. B. Pearse and A. G. Gaydon, *The Identification of Molecular Spectra*, 4th ed. (Chapman & Hall, 1976), pp. 264–265.
- ²⁴L. C. Lee, *J. Chem. Phys.* **72**, 4334 (1980).
- ²⁵O. Dutuit, A. TabcheFouhaile, I. Nenner, H. Frohlich, and P. M. Guyon, *J. Chem. Phys.* **83**, 584 (1985).
- ²⁶L. C. Lee, L. Oren, E. Phillips, and D. L. Judge, *J. Phys. B* **11**, 47 (1978).
- ²⁷S. Q. Xu, X. Sun, B. Zeng, W. Chu, J. Zhao, W. Liu, Y. Cheng, Z. Z. Xu, and S. L. Chin, *Opt. Express* **20**, 299 (2012).
- ²⁸S. Tsurubuchi, *Chem. Phys.* **10**, 335 (1975).